ACS Photonics

pubs.acs.org/journal/apchd5

Letter

Chip-Scale Integration of Nanophotonic-Atomic Magnetic Sensors

Yoel Sebbag, Alex Naiman, Eliran Talker, Yefim Barash, and Uriel Levy*

Cite This: https://dx.doi.org/10.1021/acsphotonics.0c01473

Read Online

ACCESS | Metrics & More | Article Recommendations

ABSTRACT: Optical magnetometers based on alkali vapors, such as rubidium, are among the most sensitive technologies for detecting and characterizing magnetic fields. Following the recent effort in miniaturizing atomic-based quantum technologies, the last years were marked by a growing interest in developing integrated quantum nanophotonic circuits for a vast range of applications. Motivated by the attractiveness of such chip-scale integration, we present and experimentally demonstrate an integrated magnetic sensing platform, based on a nanophotonic-chip interfaced to a microfabricated alkali vapor cell. Magnetically induced circular dichroism in rubidium vapor is measured using a planar structure that spatially resolves the handedness of incoming photons depending on their spin. The presented approach paves the way toward further integration of highly sensitive magnetometers, with potential for future applications, such as in high-spatial resolution magnetic vectorial imaging.

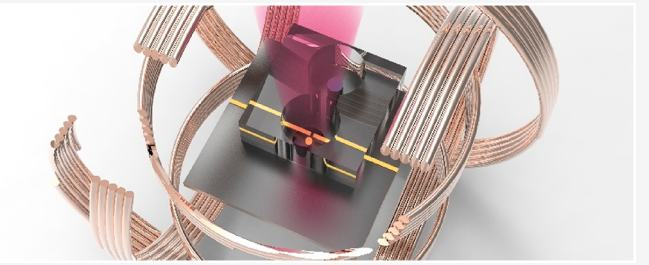

KEYWORDS: *integrated photonic, dielectric nanoantenna, atomic physics, magnetometry*

Chip-scale integration of atomic vapors with photonic systems provides a fundamental building block for quantum devices and sensors. Alkali vapors, such as rubidium (Rb), are extensively being used in several important fields of research and applications such as slow and stored light,[1] nonlinear optics,[2] quantum computation,[3] generation of single-photons,[4] radio frequency detection,[5] atomic clocks,[6] or magnetometry.[7] Several miniaturized rubidium systems have been demonstrated over the past few years, including atomic-cladded waveguide,[8−13] antiresonant hollow core waveguide,[14] and coupled atomic-plasmonic systems.[15−17] Aside from providing a path toward mass production, the high level of integration of these chip-scale configurations greatly enhances light−vapor interactions. As an example, tight confinement of light in a nanoscale waveguide can lead to strong atom-light interactions enhancing nonlinear processes, paving the way for applications such as few photons communication system by all-optical switching.[8]

However, integration and miniaturization come at a price, and the extreme confinement of light in an atomic cladded waveguide is typically followed by broadening due to short time interactions (transit time broadening), increased Doppler broadening (due to large photon momentum), and Van der Waals position-dependent shift.[8] In order to develop an efficient miniaturized atomic nanophotonic chip with performance competing with its free-space equivalent, one needs to circumvent these issues. Doing so, two research paths are explored. The first is to develop a fully integrated solution such as a nanophotonic tapered waveguide with a larger optical mode,[18] analogous of tapered fibers. A fully integrated platform has the advantage of higher miniaturization, smaller footprint, and dense integration of more devices on a single chip. However, the high confinement of the light in this platform imposes a short interaction time with the atoms, which may limit some applications.

Alternatively, one may take advantage of the cladding vapor chamber to achieve free-space interactions where the light is coupled in and out of the chip using grating couplers. In this case, additional optical elements, for example, mirrors, should be used to couple the light back to the photonic chip.[19,20] The main advantage of this approach is the straightforward implementation of a free-space layout, but this comes at the expense of complexity, a lower degree of integration, and also losing the ability to tailor the properties of the light field, for enhanced light−vapor interactions.

Highly sensitive alkali-based optical magnetometers rely on the ability to precisely control and detect the state of polarization of light. In integrated devices, the magneto-optic rotation requires precise phase matching between the TE and TM modes of the waveguide,[21] which is challenging to be achieved in highly confined asymmetric waveguides. To circumvent this challenge, we have adopted a hybrid approach and demonstrated an integrated hybrid platform for chip-scale

Received: September 22, 2020

alkali-based magnetometers, in which a microfabricated Rb cell is interfaced with a photonic chip. The magnetic sensing scheme used here is based on magnetically induced circular dichroism in Rb, in which two orthogonal circular polarizations are experiencing a large difference in their absorption spectrum in the presence of a magnetic field.[22,23] The information imprinted on each circular polarization is then retrieved using an integrated guided wave photon spin sorter (PSS), which spatially resolves the handedness of the incident photons by driving them toward different waveguides, depending on their spin. The presented platform can be further expanded, and an array of PSS can be integrated on-chip, providing a path for future applications in high spatial resolution magnetometry, near-field vectorial imaging, or magnetically induced switching and tuning.

RESULTS

Design and Characterization of PSS. The general idea behind the optical measurement of a magnetic field using atoms can be summarized as follows. Prior to the interaction, the atomic spins are randomly oriented. These spins can be aligned using a nearly resonant light beam, which polarizes the atomic spins to a long-lived ground substate by optical pumping. Then, this oriented atomic state undergoes Larmor spin precession under the ambient magnetic field. This precession modifies the optical absorptive and dispersive properties of the atomic medium and can be measured by recording the changes in the transmitted light. Highly sensitive schemes are based on nonlinear magneto optic rotations (NMOR), reaching a sensitivity as low as a few femtotesla,[24] even in 1 mm long miniaturized Rb cells.

The basic principle of NMOR-based magnetometers is based on measuring the change of the state of polarization of the light interacting with the atomic ensemble, as a function of the magnetic field. In free space, measuring the polarization rotation (magnetically induced circular birefringence) is straightforward using a half-waveplate and a polarization beam splitter. An alternative way is to measure the change of ellipticity of the interacting light (induced by magnetically dependent circular dichroism) by differentiating the signals of left and right circularly polarized light.[25]

Measuring circular dichroism in an integrated platform can be achieved using a PSS, which discriminates the handedness of incoming photons and spatially separates them depending on their spin. Our PSS device, presented in Figure 1a, consists of a single dielectric nanoantenna, supporting an electric Mie dipolar resonance at the wavelength of interaction with the D_2 line of Rb (780 nm), coupled to a waveguide by near-field interference. The nanoantenna, when excited by a circularly polarized light, acts as a rotating electric dipole, resulting in unidirectional excitation of a waveguide mode.[26] Our device was fabricated on a standard silicon wafer with a 250 nm thick silicon nitride layer grown on a 2 μm thick thermal oxide. The radius of the nanoantenna is about 300 nm. The separation from the middle of the waveguide to the close edge of the antenna is 300 nm, and the gap between the waveguides is 400 nm. These parameters were determined by finite-difference-time-domain (FDTD) simulation.

The device was characterized by focusing a light beam from the top. The polarization of the incident beam was varied using a linear polarizer (LP) and a rotating quarter waveplate (QWP) prior to the focusing objective, as shown in Figure 1b. Doing so, the polarization of the incident light can be varied

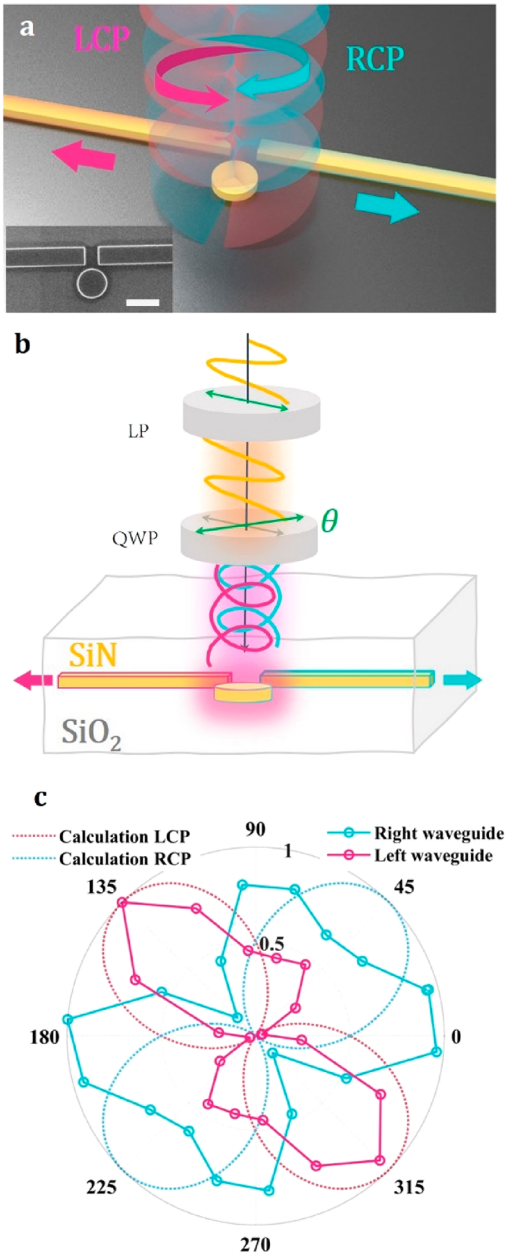

Figure 1. (a) Sketch presenting the principle of operation of the PSS, which spatially distinguishes the incoming photons depending on their spin. The inset shows a scanning electron microscope image of the fabricated device, with a 1 μm scale bar. (b) Sketch of the experimental setup for characterization of the device. (c) Experimentally measured intensity at the output of the two waveguides as a function of the angle between the QWP and LP axes. The components of RCP and LCP as calculated from the Jones calculus are also presented.

from linear polarization to right circular (RCP) or left circular polarization (LCP), depending on the relative angle between the fast axis of the QWP and the LP.

The intensity at the output of both waveguides was measured and plotted as a function of the relative angle between the LP and the QWP. The result, depicted in Figure 1c, shows a typical $\sin^2(\theta)$ dependency of the collected intensities, showing that the RCP component of the incident light is mostly coupled to the "right" waveguide, whereas the LCP component of the incident light is mostly coupled to the

https://dx.doi.org/10.1021/acsphotonics.0c01473
ACS Photonics XXXX, XXX, XXX−XXX

"left" waveguide. For comparison, the RCP and LCP components at the output of the QWP, calculated using Jones matrix are also presented. Despite the imperfection in creating a pure circular polarization, we found a good agreement between the measured output and the calculation. The discrepancy observed in the experiment may be attributed to interferences due to a misalignment of the optical setup, the generation of imperfect circular polarization by using the QWP, and fabrication imperfections. The latter case might lead to crosstalk between the output of the waveguides.

Microfabricated Cell. In order to interface the Rb vapor cell with the PSS, we have constructed a micromachined silicon-glass vapor cell, as shown in Figure 2a. The cell consists

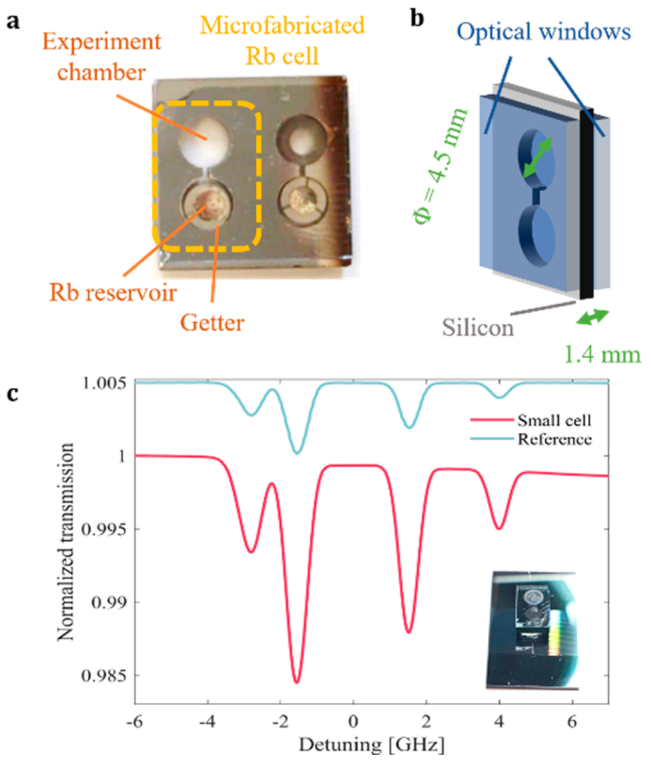

Figure 2. (a) Picture of two Rb cells, prior to cutting, showing the interaction chamber and dispenser chamber with a Rb reservoir pill and a ring-shaped getter. (b) Sketch of the Rb vapor cell presenting its dimensions. (c) Measured transmission spectroscopy through the cell, presenting the D_2 lines of naturally abundant Rb vapors in our cell, compared to the absorption in a 7 cm long reference cell at room temperature (not to scale). The inset in (c) shows a photograph of the cell on top of the photonic chip.

of a 1.4 mm thick silicon frame in which two chambers are drilled all the way through the silicon and are connected by a single channel. The chambers are round, with a diameter of 4.2 mm, as illustrated in Figure 2b, and they are designed to have a clear optical access. In one chamber, a rubidium dispenser pill is inserted, as well as a ring-shaped getter. The Rb cell is then sealed, using two borosilicate windows that are anodically bonded inside a custom-made vacuum chamber at about 10^{-9} Torr. Finally, the Rb is heat-activated by focusing a 1.5 W diode laser at 830 nm onto the pill for a time duration of 10–20 s. Another version of the cell, containing a second getter inserted in the Rb interaction chamber is also presented in Figure 2a. The measured spectroscopy of the cell, presenting the D_2 resonant lines of naturally abundant Rb, is shown in Figure 2c. The cell is then placed on top of the photonic chip (inset in Figure 2c) for magneto-optic measurements. In the future, the Rb cell can be directly integrated on the chip, for example, by direct glass-to-silicon wafer bonding.[27]

Circular Dichroism Measurements. Next, we check the ability of the PSS to measure circular dichroism induced in the Rb vapor cell. Figure 3a shows the experimental setup, in which a linearly polarized light, resonant with the D_2 line of Rb, is sent through the cell into the photonic chip. A uniform magnetic field of about 400 G was applied, parallel to the light propagation direction, using two ring-shaped neodymium permanent magnets. The light was focused onto the PSS nanoantenna using a 5× microscope objective with a numerical aperture of 0.14. The incident light was focused to a spot size of about 7 μm diameter, which covers uniformly the nanoantenna and a part of the coupling waveguides. In the future, a metalens can also be integrated into the device, eliminating the need for an external microscope objective and a complex alignment. In fact, a metalens with a focal distance of a few millimeters operating in this spectral range was recently demonstrated by our group.[28] After an interaction with the Rb vapor, the information contained in the RCP and LCP lights was spatially separated by the PSS and coupled to the opposite waveguides. The light was collected at the output of the photonic chip by lensed fibers and sent to a detector. Two polarization beam splitter fibers were connected, prior to the detector (not shown in Figure 3a), in order to select only the light coupled to the fundamental transverse electric mode of the waveguides. The measured spectroscopy at the output of each waveguide is presented in Figure 3b. The different spectra sensed by photons, depending on their spin can be efficiently retrieved. The graph also shows the theoretical spectra, calculated by solving the optical Bloch equations. The good agreement between the measured results and the theory can be observed. Also, despite the large illumination, polarization insensitive coupling by near-field scattering directly to the waveguide is negligible.[26] This measurement shows that the integrated device can be used to efficiently discriminate between the RCP and LCP components of the linearly polarized light, acting as an integrated photonic spin sorter. The measured spectra can be also differentiated to obtain the typical error signal used in dichroic atomic vapor laser locking technique,[29] as presented in Figure 3c.

Magnetic-Field Measurements in a Microfabricated Cell. Finally, we turn into the magnetic field measurements. A schematic drawing of the experimental setup is presented in Figure 4.a, in which the atomic-photonic chip is placed inside a set of custom-made Helmholtz coils in order to minimize the ambient magnetic field. In this experiment, the cell was heated to about 90 °C and a nearly resonant linearly polarized laser beam is focused onto the PSS after interaction with the Rb atoms. The light was collected at the output of the waveguides and the difference signal was recoded, as a function of the magnetic field, which was scanned around zero, in the direction of light propagation. The characteristic dispersive shaped curve is presented in Figure 4b. The linear, central portion of this curve can be used for measuring the ambient magnetic field, where the measured circular dichroism is directly proportional to the magnetic field.

The presented signal-to-noise ratio (SNR) can be further improved by minimizing the mechanical instabilities, for example, by gluing the collecting fibers,[19] and also by using magnetic shielding, in addition to the Helmholtz coils.[23,24]

https://dx.doi.org/10.1021/acsphotonics.0c01473
ACS Photonics XXXX, XXX, XXX−XXX

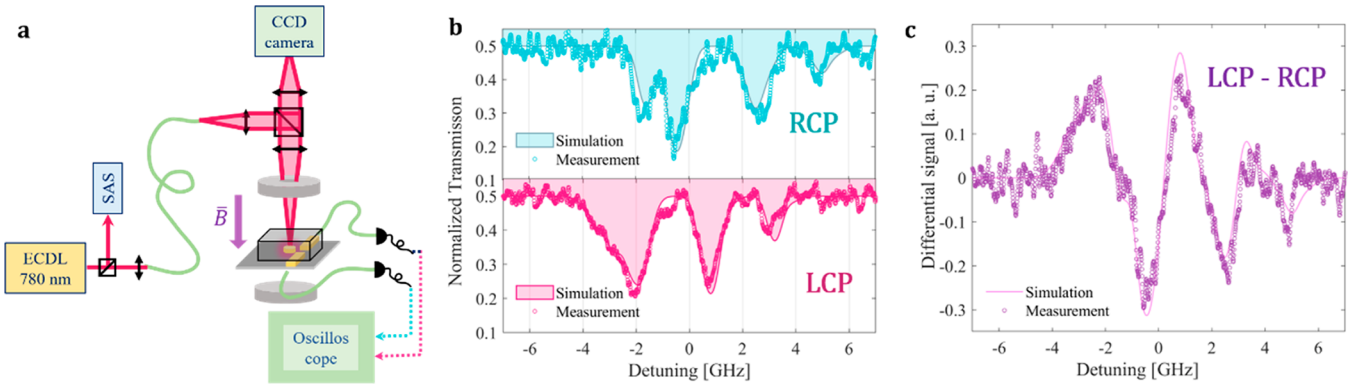

Figure 3. (a) Sketch of the experimental setup in which two permanent magnets are used to generate a uniform magnetic field of 400 G. (b) Experimental and theoretical transmission spectroscopy of Rb at the output of the device showing spatially resolved signal from the RCP (upper graph) and LCP (lower graph) components of the linearly polarized input light. (c) The error signal obtained by subtracting the normalized signals, presenting the typical dispersive shape.

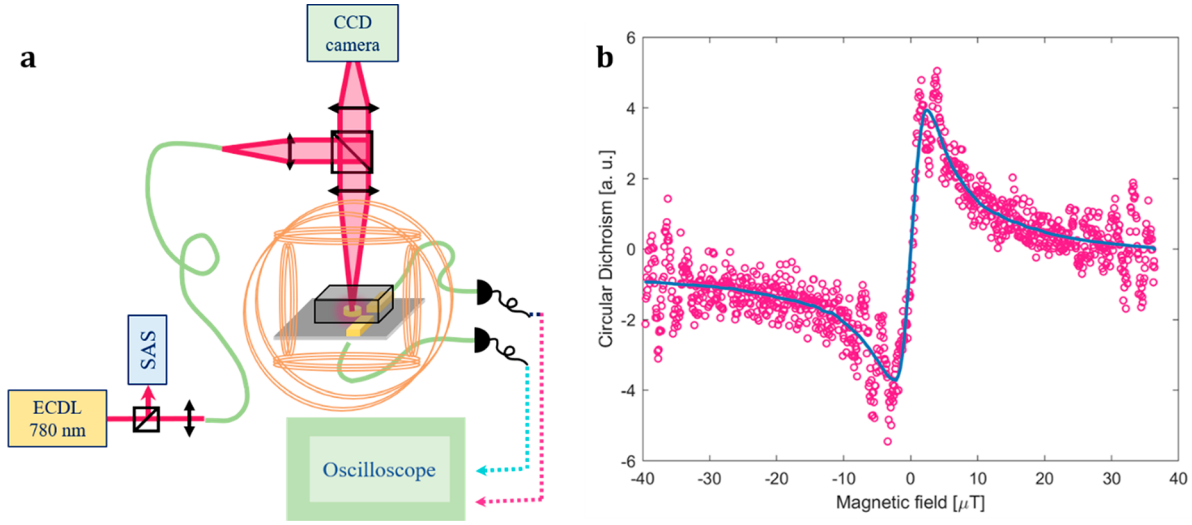

Figure 4. (a) Sketch of the experimental setup in which the device is measured inside Helmholtz coils. (b) Measured circular dichroism presenting the typical dispersive shape of NMOR. The solid blue line is a fitting curve.

Furthermore, the SNR can be improved by increasing the collection efficiency of the nanoantenna, either by tight focusing on the disk nanoantenna or by using a different geometry. Other approaches can be used to implement an efficient PSS, for example using inverse design method.

DISCUSSION AND CONCLUSION

In summary, we have demonstrated an integrated platform for measuring nonlinear magneto-optic rotation in alkali vapors. This platform consists of a microfabricated Rb cell implemented on top of a photonic chip. The magnetically induced circular dichroism in Rb atoms is detected using a single dielectric nanoantenna coupled to a waveguide, acting as an integrated photonic spin sorter (PSS). Overall, miniaturization and integration of advanced sensing schemes that are relying on polarization-dependent light−matter interaction requires the development of new concepts and techniques, which are not based on traditional bulky and discrete optical components, such as linear retarders, polarizers, and quarter-wave plates. The optical response of nanostructures can be used to develop integrated polarimeters with a reduced footprint.[26,30]

Our demonstration of an integrated magnetic quantum sensor based on hot alkali vapors is an important step toward the development of fully integrated quantum sensors and systems. Potential applications can range from a nanophotonic chip for quantum magnetic sensing, to even more challenging devices such as integrated cold atoms chip, where an integrated dichroic atomic vapor laser locking technique can be used as a part of the integrated laser cooling system. In the future, micrometer to nanometer rubidium cells can also be implemented on chip, providing even higher spatial resolution, paving the way for development of high spatial resolution near-field mapping of magnetic fields and the microscale and perhaps even the nanoscale.

AUTHOR INFORMATION

Corresponding Author

Uriel Levy − *Department of Applied Physics, the faculty of Science, the Center for Nanoscience and Nanotechnology, the Hebrew University of Jerusalem, Jerusalem 91904, Israel*; Email: ulevy@mail.huji.ac.il

https://dx.doi.org/10.1021/acsphotonics.0c01473
ACS Photonics XXXX, XXX, XXX−XXX

Authors

Yoel Sebbag − *Department of Applied Physics, the faculty of Science, the Center for Nanoscience and Nanotechnology, the Hebrew University of Jerusalem, Jerusalem 91904, Israel;* orcid.org/0000-0001-7265-6752

Alex Naiman − *Department of Applied Physics, the faculty of Science, the Center for Nanoscience and Nanotechnology, the Hebrew University of Jerusalem, Jerusalem 91904, Israel*

Eliran Talker − *Department of Applied Physics, the faculty of Science, the Center for Nanoscience and Nanotechnology, the Hebrew University of Jerusalem, Jerusalem 91904, Israel*

Yefim Barash − *Department of Applied Physics, the faculty of Science, the Center for Nanoscience and Nanotechnology, the Hebrew University of Jerusalem, Jerusalem 91904, Israel*

Complete contact information is available at: https://pubs.acs.org/10.1021/acsphotonics.0c01473

Notes

The authors declare no competing financial interest.

■ ACKNOWLEDGMENTS

Y.S. acknowledges a fellowship from the center for nanoscience and nanotechnology at the Hebrew University. The research was supported in parts by the Israeli science foundation (ISF).

■ REFERENCES

(1) Camacho, R. M.; Vudyasetu, P. K.; Howell, J. C. Four-Wave-Mixing Stopped Light in Hot Atomic Rubidium Vapour. *Nat. Photonics* **2009**, *3* (2), 103−106.

(2) Venkataraman, V.; Saha, K.; Gaeta, A. L. Phase Modulation at the Few-Photon Level for Weak-Nonlinearity-Based Quantum Computing. *Nat. Photonics* **2013**, *7* (2), 138−141.

(3) Lvovsky, A. I.; Sanders, B. C.; Tittel, W. Optical Quantum Memory. *Nat. Photonics* **2009**, *3* (12), 706−714.

(4) Ripka, F.; Kübler, H.; Löw, R.; Pfau, T. A Room-Temperature Single-Photon Source Based on Strongly Interacting Rydberg Atoms. *Science* **2018**, *362* (6413), 446−449.

(5) Sedlacek, J. A.; Schwettmann, A.; Kübler, H.; Löw, R.; Pfau, T.; Shaffer, J. P. Microwave Electrometry with Rydberg Atoms in a Vapour Cell Using Bright Atomic Resonances. *Nat. Phys.* **2012**, *8* (11), 819−824.

(6) Knappe, S.; Shah, V.; Schwindt, P. D. D. D.; Hollberg, L.; Kitching, J.; Liew, L.-A. A.; Moreland, J. A Microfabricated Atomic Clock. *Appl. Phys. Lett.* **2004**, *85* (9), 1460−1462.

(7) Kitching, J. *Chip-Scale Atomic Devices*; American Institute of Physics Inc., 2018; Vol. *5*, p 31302.

(8) Stern, L.; Desiatov, B.; Mazurski, N.; Levy, U. Strong Coupling and High-Contrast All-Optical Modulation in Atomic Cladding Waveguides. *Nat. Commun.* **2017**, *8*, 14461.

(9) Ritter, R.; Gruhler, N.; Pernice, W.; Kübler, H.; Pfau, T.; Löw, R. Atomic Vapor Spectroscopy in Integrated Photonic Structures. *Appl. Phys. Lett.* **2015**, *107* (4), 041101.

(10) Stern, L.; Desiatov, B.; Goykhman, I.; Levy, U. Nanoscale Light-Matter Interactions in Atomic Cladding Waveguides. *Nat. Commun.* **2013**, *4*, 1548.

(11) Ritter, R.; Gruhler, N.; Pernice, W. H. P.; Kübler, H.; Pfau, T.; Löw, R. Coupling Thermal Atomic Vapor to an Integrated Ring Resonator. *New J. Phys.* **2016**, *18* (10), 103031.

(12) Stern, L.; Zektzer, R.; Mazurski, N.; Levy, U. Enhanced Light-Vapor Interactions and All Optical Switching in a Chip Scale Micro-Ring Resonator Coupled with Atomic Vapor. *Laser Photon. Rev.* **2016**, *10* (6), 1016−1022.

(13) Zektzer, R.; Talker, E.; Barash, Y.; Mazurski, N.; Levy, U. Chiral Light-Matter Interactions in Hot Vapor-Cladded Waveguides. *Optica* **2019**, *6* (1), 15.

(14) Yang, W.; Conkey, D. B.; Wu, B.; Yin, D.; Hawkins, A. R.; Schmidt, H. Atomic Spectroscopy on a Chip. *Nat. Photonics* **2007**, *1* (6), 331−335.

(15) Stern, L.; Grajower, M.; Levy, U. Fano Resonances and All-Optical Switching in a Resonantly Coupled Plasmonic-Atomic System. *Nat. Commun.* **2014**, *5*, 4865.

(16) Aljunid, S. A.; Chan, E. A.; Adamo, G.; Ducloy, M.; Wilkowski, D.; Zheludev, N. I. Atomic Response in the Near-Field of Nanostructured Plasmonic Metamaterial. *Nano Lett.* **2016**, *16* (5), 3137−3141.

(17) Stern, L.; Grajower, M.; Mazurski, N.; Levy, U. Magnetically Controlled Atomic-Plasmonic Fano Resonances. *Nano Lett.* **2018**, *18* (1), 202−207.

(18) Zektzer, R.; Mazurski, N.; Barash, Y.; Levy, U. Tapered Atomic Cladded Nano Waveguide for Fine Control of Light-Atom Interaction. *Conference on Lasers and Electro-Optics*; OSA: Washington, D.C., 2019; p FF3M.5.

(19) Hummon, M. T.; Kang, S.; Bopp, D. G.; Li, Q.; Westly, D. A.; Kim, S.; Fredrick, C.; Diddams, S. A.; Srinivasan, K.; Aksyuk, V.; et al. Photonic Chip for Laser Stabilization to an Atomic Vapor with 10−11 Instability. *Optica* **2018**, *5* (4), 443.

(20) Bopp, D.; Kang, S.; Hummon, M.; Kitching, J.; Kim, S.; Yulaev, A.; Srinivasan, K.; Westley, D.; Aksyuk, V. Nanophotonic Integration of Atomic Wavelength References. *Conference on Lasers and Electro-Optics*; OSA, 2019; p STu4G.4.

(21) Tien, P. K.; Schinke, D. P.; Blank, S. L. Magneto-Optics and Motion of the Magnetization in a Film-Waveguide Optical Switch. *J. Appl. Phys.* **1974**, *45* (7), 3059−3068.

(22) Bloom, A. L. Principles of Operation of the Rubidium Vapor Magnetometer. *Appl. Opt.* **1962**, *1* (1), 61.

(23) Kominis, I. K.; Kornack, T. W.; Allred, J. C.; Romalis, M. V. A Subfemtotesla Multichannel Atomic Magnetometer. *Nature* **2003**, *422* (6932), 596−599.

(24) Griffith, W. C.; Knappe, S.; Kitching, J. Femtotesla Atomic Magnetometry in a Microfabricated Vapor Cell. *Opt. Express* **2010**, *18* (26), 27167.

(25) Marcis, A.; Budker, D.; Rochester, S. *Optically Polarized Atoms*; Oxford University Press: New York, NY, 2010.

(26) Rodríguez-Fortuño, F. J.; Barber-Sanz, I.; Puerto, D.; Griol, A.; Martínez, A. Resolving Light Handedness with an On-Chip Silicon Microdisk. *ACS Photonics* **2014**, *1* (9), 762−767.

(27) Chen, T.; Sun, L.; Pan, M.; Wang, Y.; Liu, J.; Chen, L. Anodic Bonding Technology of Slender Glass Tube and Silicon in Pressure Sensor Packaging. *Proceedings of the 2013 IEEE 15th Electronics Packaging Technology Conference, EPTC 2013* **2013**, 813−816.

(28) Engelberg, J.; Zhou, C.; Mazurski, N.; Bar-David, J.; Kristensen, A.; Levy, U. Near-IR Wide-Field-of-View Huygens Metalens for Outdoor Imaging Applications. *Nanophotonics* **2020**, *9* (2), 361−370.

(29) Corwin, K. L.; Lu, Z.-T.; Hand, C. F.; Epstein, R. J.; Wieman, C. E. Frequency-Stabilized Diode Laser with the Zeeman Shift in an Atomic Vapor. *Appl. Opt.* **1998**, *37* (15), 3295.

(30) Martínez, A. Polarimetry Enabled by Nanophotonics. *Science* **2018**, *362* (6416), 750−751.

https://dx.doi.org/10.1021/acsphotonics.0c01473
ACS Photonics XXXX, XXX, XXX−XXX